

Simulation Standard

Connecting TCAD To Tapeout

A Journal for Process and Device Engineers

Using ATHENA Monte Carlo Module for Ion Implantation Simulation in Silicon Carbides

Introduction

The Monte Carlo Implantation Module of *ATHENA* has proved to be a very accurate tool for simulation of various implantation processes. In this paper we demonstrate that the module can be successfully used not only for classical silicon-based technologies but also for other materials used in semiconductor industry. Silicon carbides were selected for this demonstration not only because they are widely used in power and high frequency electronics but also because they are most challenging objects for simulation due to their complicated lattice structures and electronic stopping models.

The large number of silicon carbide (SiC) polymorphic types (more than 150) presents a variety of physical properties, some of them critically important for fabrication of power devices. For example, the 4H polytype of SiC with a band gap of 3.27 eV and electron mobility almost twice that of 6H-SiC is a material of immense interest for production of power and high frequency devices. Ion implantation as well as related effects including damage formation, amorphization, dopant activation and annealing play an important role in fabrication of planar devices in semiconductors. These components of device processing are even more critical for SiC-based technologies because extremely low impurity diffusivities are typical in SiC and therefore ion implantation becomes the only practical selective-area doping method.

The implementation of ion implantation processing is one of the key challenges in silicon carbide device fabrication. The crystal structure of the polymorphic 4H type has wide openings in certain crystallographic directions, e.g. [11-23] and [11-20], potentially giving rise to deep ion channeling effects. For example, implantation of aluminium in the [11-23] direction results in a channeled profile, which is three times deeper compared to implantation with normal incidence and five times deeper compared to an implant off major axis

(or "random") direction. Besides, to facilitate epitaxial growth, most commercial (0001) wafers are offered with 3.5° to 8.5° miscut, therefore ion implantation performed in the normal direction to such wafers corresponds to a "random" direction. Given the directional complexity of 4H-SiC and 6H-SiC structures, it is extremely difficult to minimize or accurately predict the channeling effects because of the proximity of open channels ([0001], [11-23] and their equivalents).

Modeling of ranges and stopping is a powerful research technique for predicting dopant profiles in crystalline materials. As channeling plays an important role in the propagation of ions in crystalline SiC, modelling is an indispensable tool for optimizing initial implant conditions and avoiding the long tails in the implanted profiles. The ion implantation simulator could also be used in optimizing the implant conditions to obtain profiles of a desired shape. For example, it is typical for SiC technology that deep box-like doping profiles are formed using multiple implant process steps with different energies and doses.

In this work we describe a modelling technique based on the Binary Collision approximation along with the physical model used in order to achieve highly predictive simulation of ion implantation in crystalline SiC targets.

Continued on page 2 ...

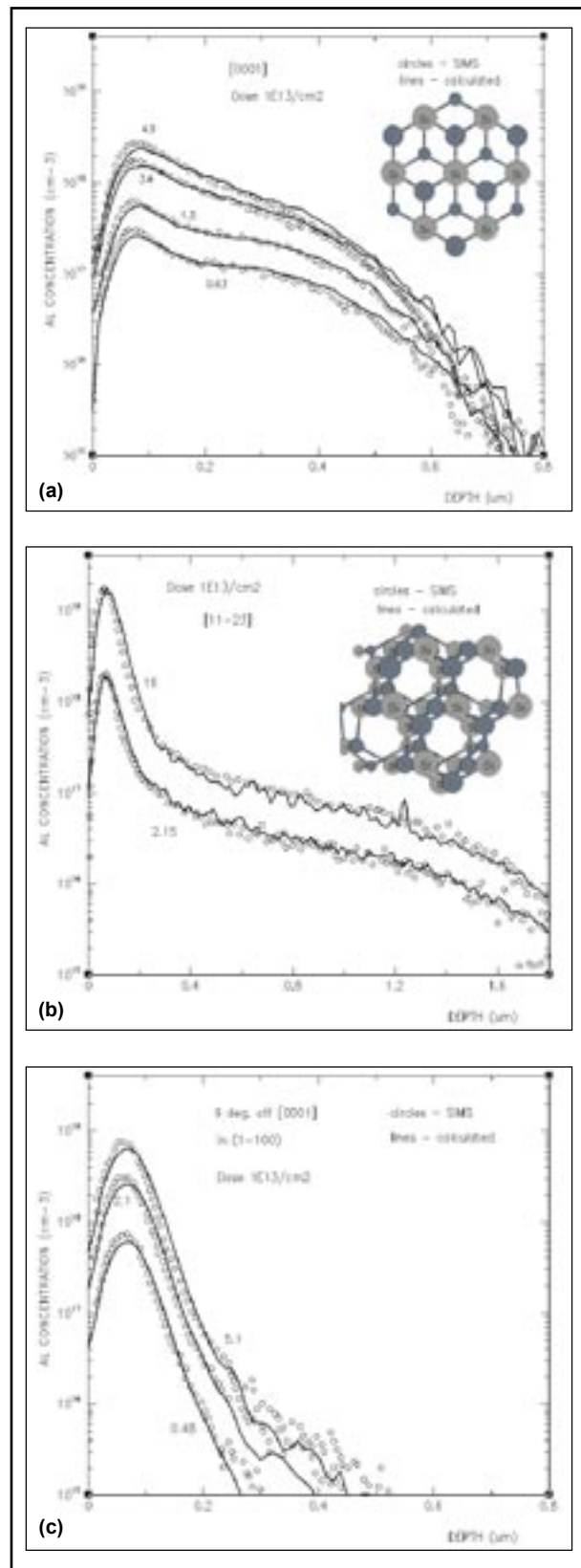
INSIDE

<i>Gate Charging Simulation Using ATLAS/MixedMode</i>	<i>6</i>
<i>Process Flow Simulation and Manufacture of Variable RF MEMS Capacitors</i>	<i>5</i>
<i>Calendar of Events</i>	<i>9</i>
<i>Hints, Tips, and Solutions</i>	<i>10</i>

Simulation Model

The Monte Carlo ion implant module uses the Binary Collision (BC) approximation a detailed description of which has been presented elsewhere, [1-3]. The principal assumption in this approximation is that the interaction of energetic particles may be separated into a series of two-body collisions. Although not exact, this close approximation replaces the real trajectory of the moving particle by straight paths between the deflection points. The important benefit of this approach is the moderate speed of calculation combined with the possibility to accurately predict effects characteristic to single crystal structures. The slowing down of energetic particles is a result of nuclear and electronic stopping. The description of target atoms uses the translational symmetry of the crystal. A list is made of the positions of target atoms in the crystal, using one of the lattice sites as the origin of co-ordinates. The crystal search procedure finds all target atoms ahead of the ion's motion with impact parameters less than p_{max} , a threshold value above which scattering is negligible. Crystal temperature is modelled by means of normally distributed displacements of the lattice atoms from their equilibrium positions. The amplitude of these displacements is evaluated with the Debye model.

Of critical importance for modelling ion implantation in crystalline targets is the electronic stopping model. Moving particles interact in a complex manner with the electrons in the target. The net effect of these interactions is velocity and position dependent retarding force acting on the moving ion. The electronic stopping in solids could be separated into two essentially different components - an electron excitation part and a continuous drag force acting on the moving particle from the surrounding electron gas. In our simulator, the value of the quasielastic electron excitation part is estimated by Firsov's model for electronic energy losses with a correction for high energies when energy transfer diminishes as described in, [4]. This is essentially a *local* inelastic energy loss because it is localized at points of closest approach in the ion-atom collisions. Thus it affects the scattering angles and the remaining energy after each collision. The other part of the electronic stopping, the so-called *non-local* inelastic energy loss, depends on the electronic density in the crystal. This electronic stopping in SiC is difficult to model due to a complex electron density distribution, see for example [5], and a complex crystal structure with many open channels and planes. Our approach is to use the stopping model of Wang, Ma and Cui, [6], with corrections for the highly anisotropic valence electron density distribution.



Discussion

The validation of the implemented model has been performed with published experimental as-implanted profiles. The compiled data were selected from articles with well explained experimental conditions. In Figure 1 are shown simulated test results for 60 keV Al implants into 4H-SiC compared to experimental profiles taken from, [7]. Wafer orientation is (0001) and the major flat has been chosen to be (1100). Implants are performed with normal incidence to the surface, Figure 1(a), or oriented along the [11-23] channel, Figure 1(b). Both profile sets show deep tails due to channeling, the profiles of Al implanted along [11-23] channel being much deeper. On the offsets in Figure 1(a)-(b) are shown the crystal structures as seen in the direction of ion implantation. The [11-23] channel is 17° off the normal in the (1-100) plane. Two factors contribute to the deep tails of the profiles in this direction, a) the well formed open channel in 4H-SiC and, b) the Z_1 dependence of the electronic stopping, S_e (see [5,8] and references therein). Under channeling conditions, $S_e(Z_1)$ has well defined oscillatory dependence. It turns out that $Z_1=13$ (aluminum) lies very close to a minimum on the $S_e(Z_1)$ curve. Therefore, aluminum ions travel much deeper along the channel than phosphorus ($Z_1=15$), [9]. Any optimization of the initial implant conditions would require correct prediction of channeled profiles. Once a satisfactory agreement of the aluminium ion distributions implanted under channeling conditions, Figure 1(a),(b), has been achieved, the final validation of the model is implantation in a 'random' direction, i.e. away from any open channel in the 4H-SiC lattice. Figure 1(c) shows such one set of profiles obtained by 9° tilt off the normal, [0001]. The model correctly predicts the peaks due to the "random" portion of ion's stopping and the tails due to the "channeling" fraction by aluminum ions occasionally entering open channels in the 4H-SiC lattice.

In Figure 2 is shown more practical application of the model for multiple Al implants into 6H-SiC. Once again, the level of agreement with the experiment can be achieved only if the range and the shape of each individual profile agrees well with the corresponding experimental one.

Conclusions

Using an appropriate electronic stopping model for SiC, one can obtain highly predictive simulation results of ion implantation within the binary collision approximation formalism. Accounting for the anisotropy of the electronic density distribution in the 4H-SiC and 6H-SiC lattices is critical for simulation of predictive implant distributions not only along open channel directions, but

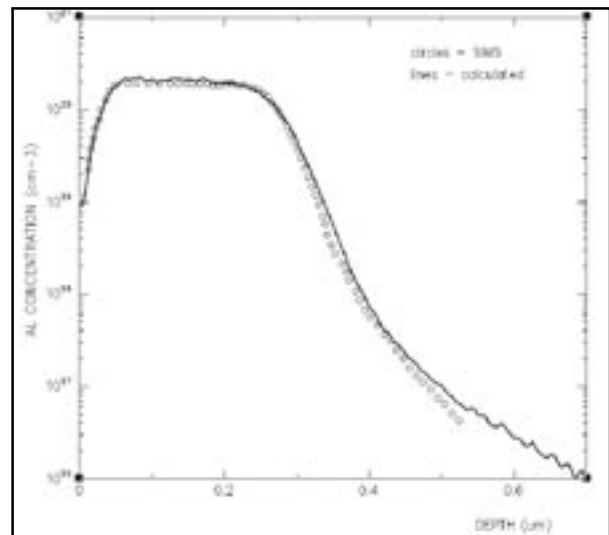


Figure 2. Box profile obtained by multiple Al implantation into 6H-SiC at energies 180, 100 and 50 keV and doses 2.7×10^{15} , 1.4×10^{15} and $9 \times 10^{14} \text{ cm}^{-2}$ respectively. The accumulated dose is $5 \times 10^{15} \text{ cm}^{-2}$. Experimental profile is taken from [10].

along "random" direction as well. The described model is implemented in the Monte Carlo Implant Module and successfully used by several *ATHENA* customers. These results were originally presented at 14th International Conference on Ion Beam Modification of Material (IBMM-2004) and will be published in the Nuclear Instruments and Methods in Physics Research B.

References

- [1] M. T. Robinson, *Radiation Effects and Defects in Solids* **130-131**, 3 (1994).
- [2] M. T. Robinson, and I. M. Torrens, *Physical Review* **B 9**, 5008 (1974).
- [3] I. R. Chakarov, and R. P. Webb, *Radiation Effects and Defects in Solids* **130-131**, 447 (1994).
- [4] M. J. van Dort, P. H. Woerlee, and A. J. Walker, *Solid-State Electronics* **37**, 411 (1994).
- [5] C. H. Park, B.-H. Cheong, K.-H. Lee, and K. J. Chang, *Physical Review* **B 49**, 4485 (1994).
- [6] Y.-N. Wang, and T.-C. Ma, *Physical Review* **A 44**, 1768 (1991).
- [7] J. Wong-Leung, M. S. Janson, and B. G. Svensson, *Journal of Applied Physics* **93**, 8914 (2003).
- [8] R. Smith, M. Jakas, D. Ashworth, B. Owen, M. Bowyer, I. Chakarov, and R. Webb, *Atomic and Ion Collisions in Solids and at Surfaces*, R. Smith Ed., Cambridge University Press, 1997.
- [9] R. G. Wilson, D. M. Jamba, P. K. Chu, C. G. Hopkins, and C. J. Hitzman, *Journal of Applied Physics* **60**, 2806 (1986).
- [10] T. Kimoto, A. Itoh, H. Matsunami, T. Nakata, and M. Watanabe, *Journal of Electronic Materials* **25**, 879 (1996).

Gate Charging Simulation Using *ATLAS/MixedMode*

Introduction

In modern power devices, the total power loss comprises both a conductive power loss component and a capacitive loss component. As the cell pitch decreases, the conductive loss will decrease while the capacitive loss will increase. Therefore, for small cell pitch the capacitive power loss may be the dominant component of the total power loss in the device.

There is clearly a need for a method that will allow analysis of the capacitive component of the power loss. One technique to do this in a power UMOSFET device is to analyze the gate charging time using *ATLAS/MixedMode*.

ATLAS/MixedMode is a circuit simulator that can include elements simulated using device simulation, as well as compact circuit models.

Device Structure and Circuit

As shown in Figure 1, this design has a U-Groove in the gate region, and has a higher channel density which reduces the on-resistance as compared to VMOSFETs or DMOSFETs.

Effects of device size and transconductance makes power loss component analysis more difficult. A more useful parameter from the circuit design point of view is the gate charge rather than capacitance. Figure 2 shows the gate charge simulation test circuit.

Simulation Results and Discussion

The advantage of using gate charge is that the designer can easily calculate the amount of current required from the drive circuit to switch the device on in a desired length of time because $Q=CV$ and $I=C dv/dt$, the gate charge is the product of time and current.

For example, a device with a gate charge of 20nC can be turned on in 20 μ s if 1mA is supplied to the gate or it can turn on in 20ns if the gate current is increased to 1A. These simple calculations would not have been possible with input capacitance values.

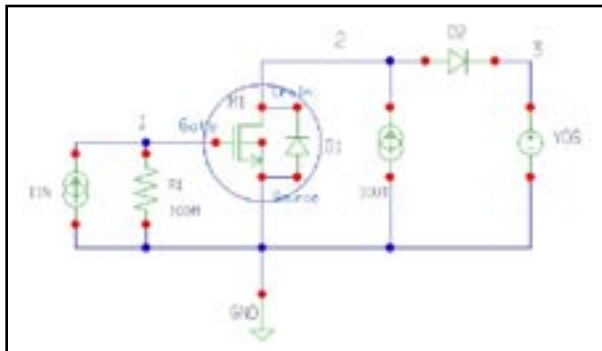


Figure 2. Test Circuit for Gate Charging

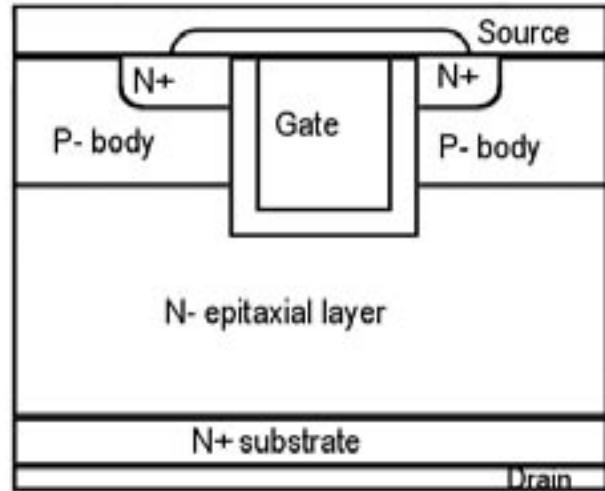


Figure 1. Typical UMOSFET Structure

Figure 3 shows gate voltage versus drain bias. From 4 μ s, drain voltage becomes $V_{ds(on)}=I_{on} \cdot R_{ds(on)}$, and the transient is completed. The MOSFET is biased to the edge of the ohmic region from the active region. From this waveform, the total gate charge, gate-source charge and gate-drain(Miller) charge can be obtained from the product of time and gate current.

Conclusion

This article presented a review of the capacitive loss of a power MOSFET using the *ATLAS/MixedMode* simulator. This gate charging analysis makes it easy to calculate the amount of current to switch the device in a desired length of time.

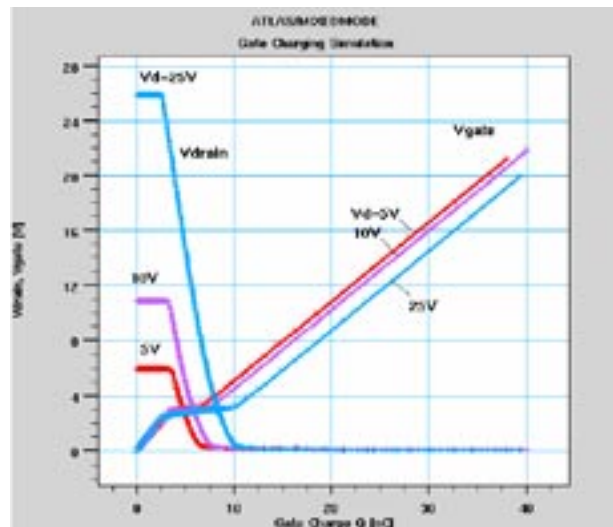


Figure 3. The waveform of the gate charging at gate current is 2mA

Process Flow Simulation and Manufacture of Variable RF MEMS Capacitors

Yong Qing Fu, Jack Luo, Stuart Milne, Andrew Flewitt
Engineering Department, University of Cambridge, Cambridge UK
Ahmed Nejm
Silvaco, St Ives, Cambridgeshire PE27 5JL, UK

Introduction

The application of microelectromechanical systems (MEMS) to radio-frequency (RF)/microwave systems is on the verge of revolutionizing wireless communications, mainly in the areas of wireless personal communication systems, wireless local area networks, satellite communications, and automotive electronics [1]. In this article we present a brief introduction to the design and fabrication effort at the Engineering Department, University of Cambridge, which is focused on variable RF capacitor MEMS structures. Silvaco 2D/3D process simulation was used to simulate the process flow and reproduce the obtained structures as a first step to future process flow and structure designs.

Variable RF capacitors with a-Si:H (doped with phosphine) cantilevers have been designed and fabricated with different length top multi-cantilever electrodes (Figure 1). This was done to produce a discrete increase of the capacitance with the applied voltage.

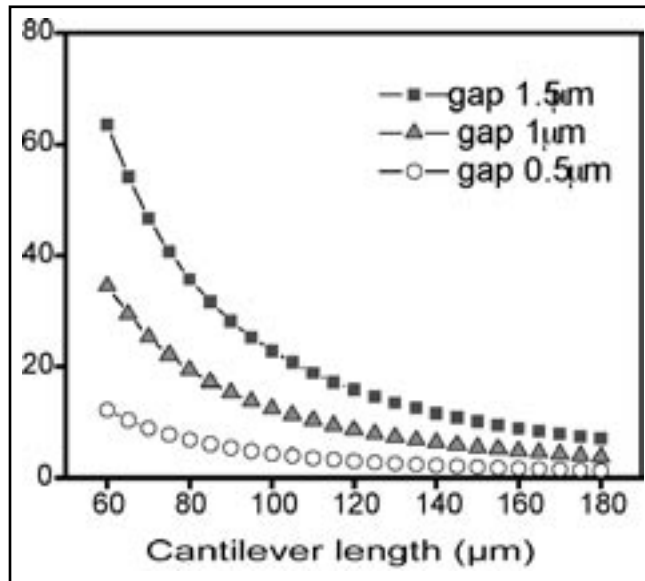


Figure 2. The calculated pull-in voltage as a function of cantilever length and air gap.

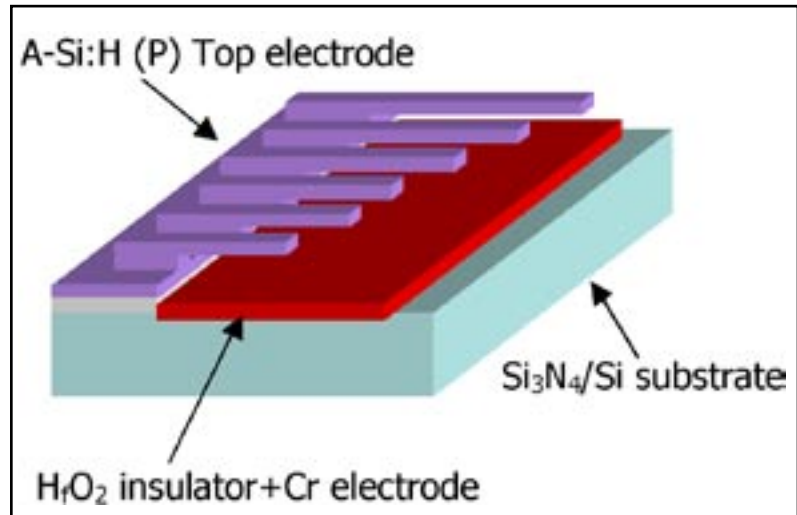


Figure 1. Schematic illustration of the variable capacitor RF MEMS switch. The top beams snap down one by one as applied voltage increase.

Increasing the applied voltage will pull down the cantilever beams sequentially. The structure consists of a bottom electrode (Cr), a top electrode (a-Si:H doped with phosphine) with suspended multi-length cantilevers overhanging on the bottom electrode, and a layer of high K material (HfO_2) as an insulating layer.

a-Si:H film was chosen for its potential for MEMS applications. The high deposition rate (as high as 100Å/s has been reported [2]), relatively low stress, and low deposition temperature (can be as low as 100°C, thus glass and plastics are applicable) [3] make it a good candidate for such applications. Add to that the good electronic properties (with phosphine and boron doped) and reasonable mechanical properties of a-Si:H film suggests that they can be used as the structural layers for thin film MEMS.

High-k material, HfO_2 , was used as an insulating layer between the bottom and top electrodes to increase the tuning range of the capacitance, because the increase in the capacitance is proportional to the dielectric constant ϵ of the insulator material.

Using the consideration of the opposite forces seen by the suspended cantilevers, the pull in voltage is defined as the threshold voltage when the mechanical restoring force can no longer balance the electrostatic force, and the

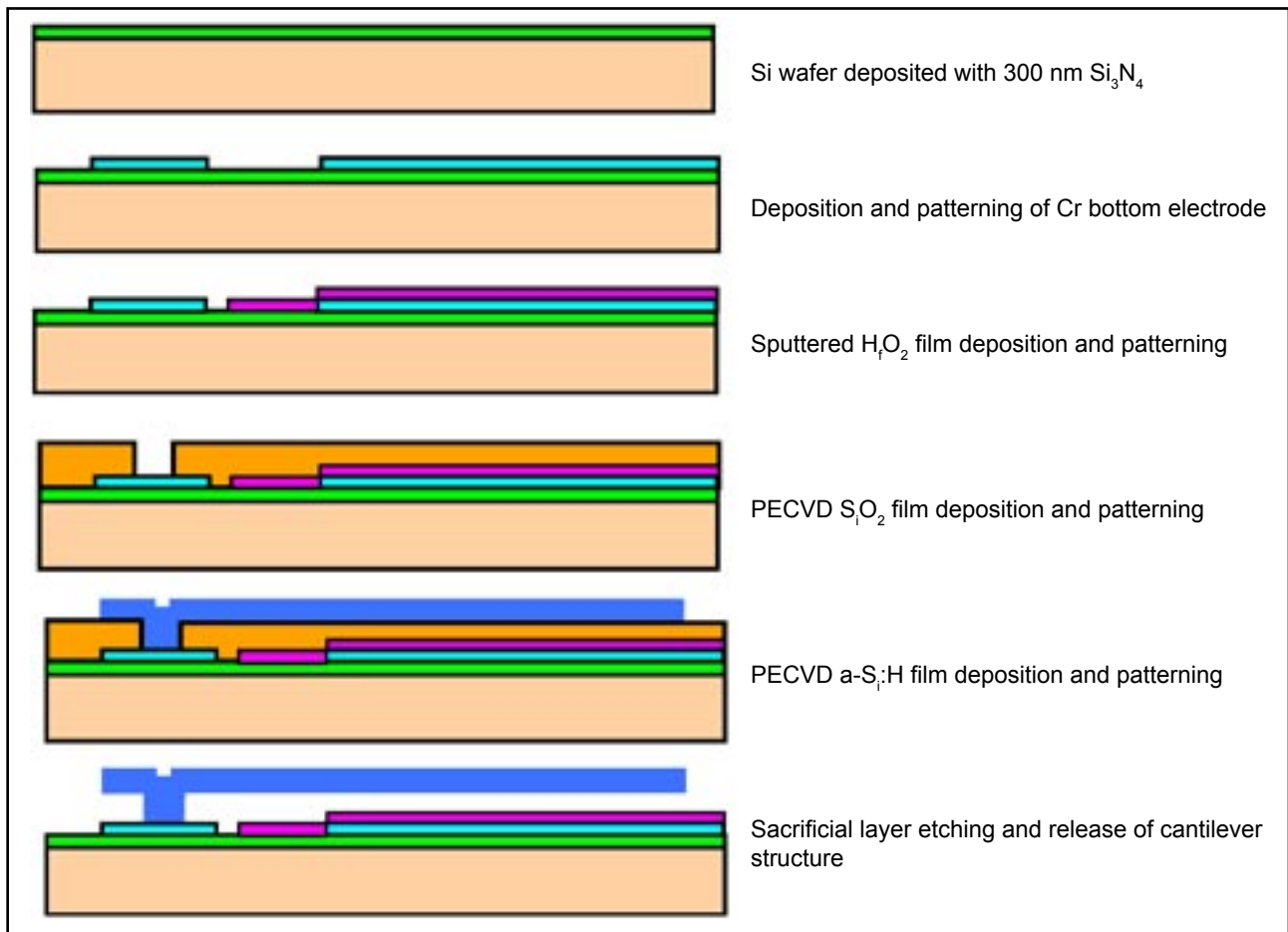


Figure 3. Schematic illustration of the fabrication process flow. Each represents a cut plane along a cantilever.

cantilever abruptly falls to the bottom contact. The calculation of these forces produced the following pull in voltage data as a function of cantilever length and the separating gap.

Fabrication Process

Figure 3 illustrates schematically the fabrication process followed to realize the cantilevers. Crucially the last step (the cantilever release) involves the sacrificial etch of the PECVD deposited oxide.

This fabrication process was simulated using Silvaco *CLEVER 3D* builder programme. The original mask set file in .cif format contained many repeated cells. Using *MaskViews* it was possible to view these masks and crop the unwanted cells. The resulting mask set was utilized in building a typical cell by following the above process flow in *CLEVER*.

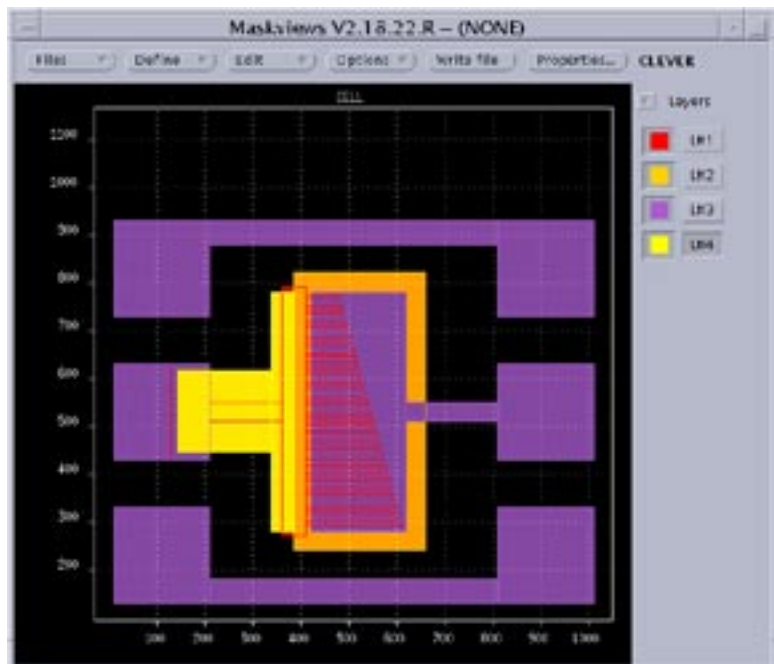


Figure 4. The cantilever mask set viewed in *MaskViews*.

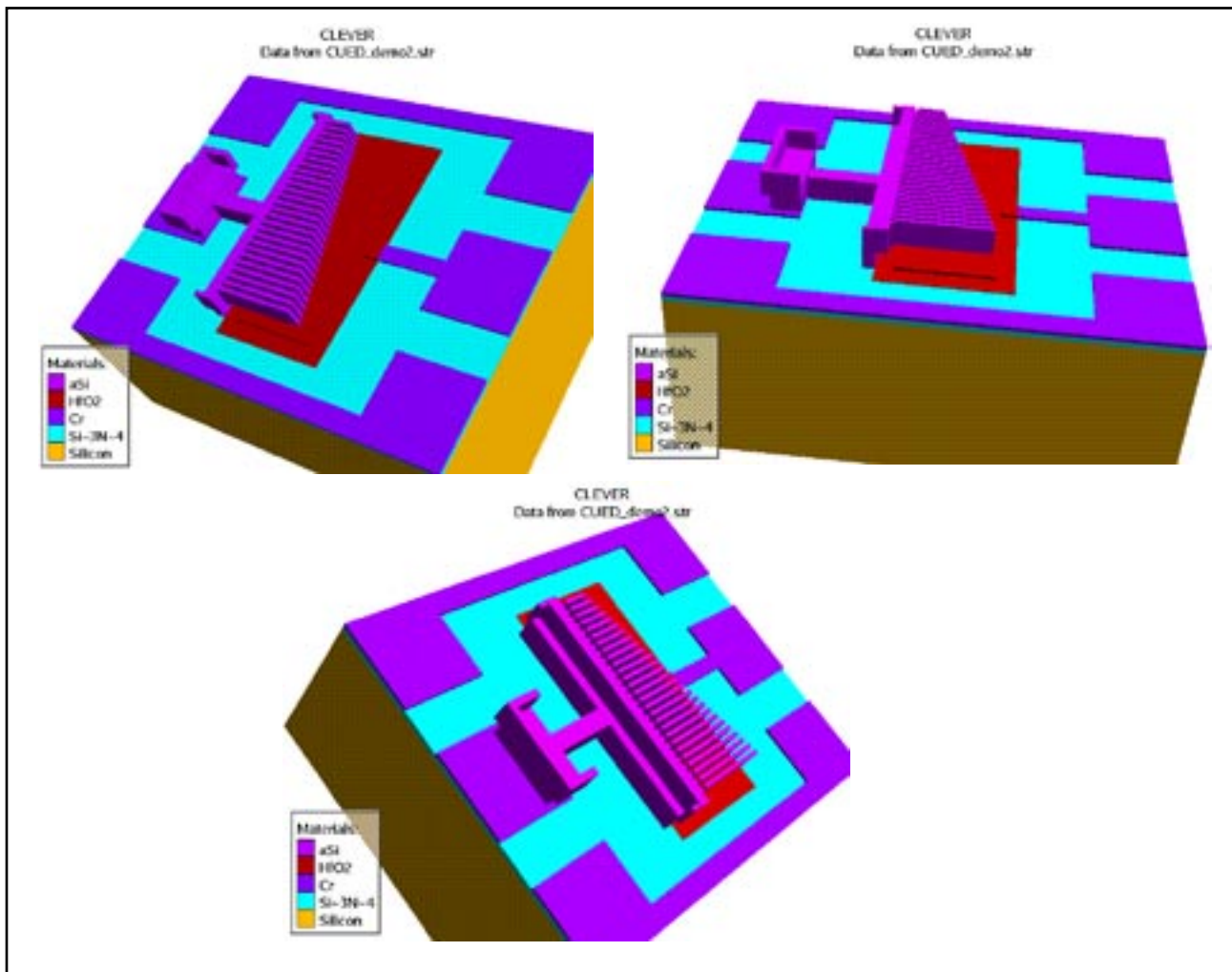


Figure 5. Results from 3D simulation of the MEMS process flow using **CLEVER**.

Once the mask set was defined the four mask process was followed as defined in Figure 3. The process culminated in the release step where all the underlying oxide is removed. The final 3D structure produced by the simulation can be seen from various points of view in Figure 5.

The cross section view obtained from a cut plane along the middle cantilever is shown in Figure 6.

The obtained data show a good match to the SEM micrographs obtained from the manufactured structures as in Figure 7.

Further details of the manufacturing process and the material analysis as well as the function of these cantilever capacitors can be found other publications [4,5].

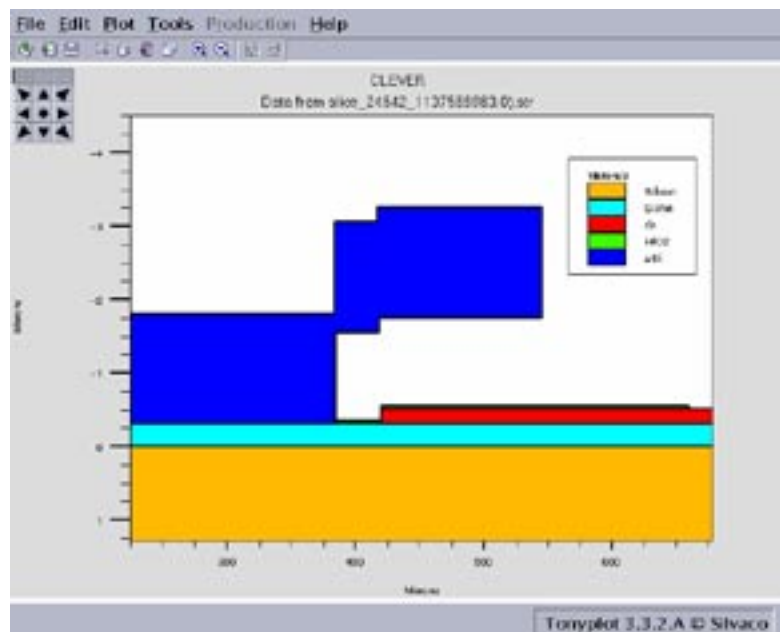


Figure 6. Cross sectional view (2D) through one of the cantilevers.

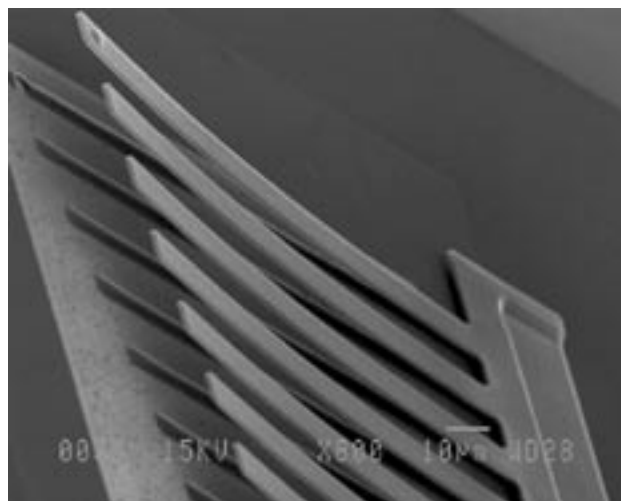
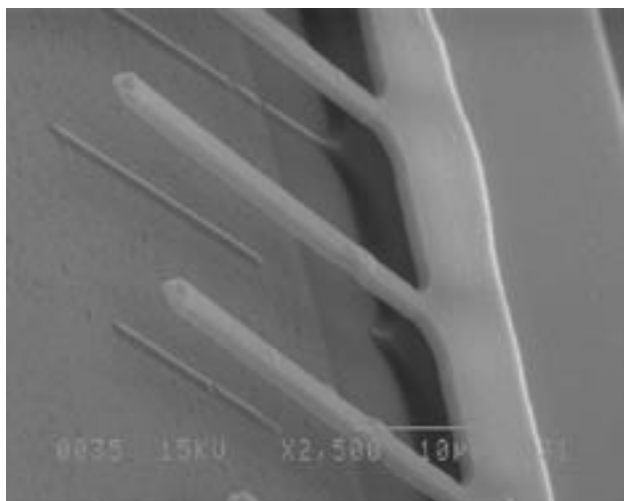
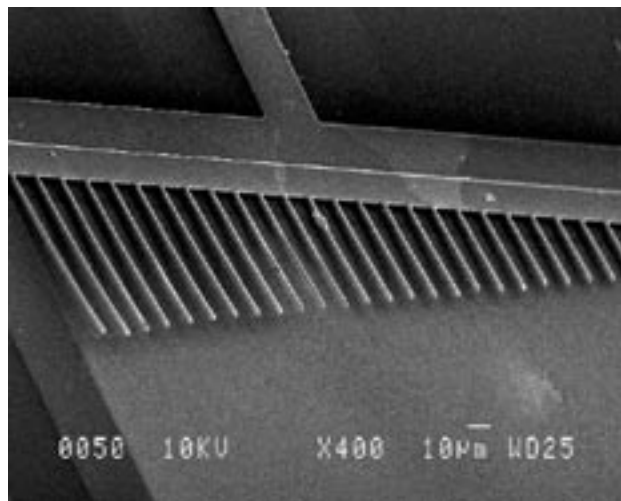
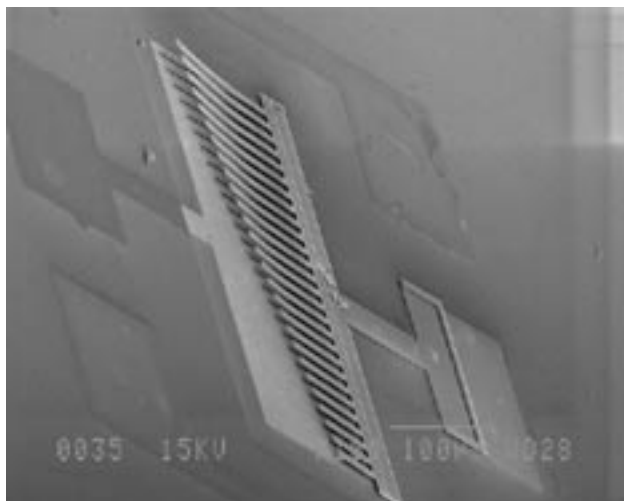


Figure 7. SEM morphologies of the fabricated capacitors with different width and lengths.

Conclusion

Using existing mask sets, it is possible to obtain good match between the manufactured variable capacitor MEMS and the 3D simulations using *CLEVER*. This is a first step in using mask design and process simulation to define future generations of these cantilever structures.

This 3D simulator has been integrated into a comprehensive design environment as part of an EU sponsored project "PROMENADE (507965)" which is coming into its testing phase.

References

- [1] H. J. D. L. Santos, G. Fisher, H. A. C. Tilmans, J. T. M. van Beek, *IEEE Microwave Mag.* 4 (2004) 36-65.
- [2] A. H. Mahan, Y. Xu, D. L. Willaimson, W. Beyer, J. D. Perkins, M. Vanecek, L. M. Gedvilas, B. P. Nelson, *J. Appl. Phys.*, 90 (2001) 5038-5047.
- [3] J. P. Conde, J. Gaspar, V. Chu, *Thin Solid Films*, 427 (2003) 181-186.
- [4] Y.Q. Fu, J. K. Luo, S. B. Milne, A. J. Flewitt, W. I. Milne, *Mater. Sci. Engng. B*, 124 (2005) 132-137.
- [5] J.K.Luo, M.Lin, Y.Q.Fu, H.Lin, A.J.Flewitt, S.M.Spearing, N.A.Fleck, W.I.Milne, MEMS digital variable capacitors with a high-k dielectric insulator, EUROSENSOR 2005, Sept. 12-15, Barcelona, Spain.

Calendar of Events

August

1
2
3
4
5
6
7
8
9
10
11
12
13
14
15
16
17
18
19
20
21
22
23
24
25
26
27
28
29
30
31

September

1
2
3
4
5
6
7
8
9
10
11
12
13
14
15
16
17
18
19 CICC
20 CICC
21
22
23
24
25
26
27
28
29
30

Bulletin Board



TMA Compatibility

Silvaco announced the availability of full TMA compatibility in its 5.10.0.R release of Stanford-based *ATHENA* Process and *ATLAS* Device Simulators. Technology Computer Aided Design (TCAD) was originally pioneered at Stanford University under grants from the Defense Advanced Research Projects Agency (DARPA) during late 1970s and 1980s. It was licensed to and commercialized exclusively by Technology Modeling Associates (TMA) and Silvaco. TMA was later acquired by Avant! Corporation which was then acquired by Synopsys. In October 2004, Synopsys also acquired Integrated Systems Engineering (ISE), a TCAD provider based in Switzerland. Synopsys announced its future TCAD products would be based on the ISE software.



Silvaco TCAD Future

Silvaco will continue to provide advanced TCAD technologies based on the latest physical models for process and device simulation. Silvaco is the only company dedicated to exclusively support the Stanford TCAD legacy. Switching to Silvaco TCAD means that TMA customers do not have to recalibrate their model coefficients, re-establish their process and device simulation flows developed over many years, and learn new software.

If you would like more information or to register for one of our workshops, please check our web site at <http://www.silvaco.com>

The Simulation Standard, circulation 18,000 Vol. 15, No. 8, August 2005 is copyrighted by Silvaco International. If you, or someone you know wants a subscription to this free publication, please call (408) 567-1000 (USA), (44) (1483) 401-800 (UK), (81)(45) 820-3000 (Japan), or your nearest Silvaco distributor.

The following trademarks and service marks are the property of Silvaco International. Registered Marks:® Virtual Wafer Fab, Silvaco. Trademarks:™ Simulation Standard, ATHENA, Analog Alliance, Legacy, Manufacturing Tools, Automation Tools, SFLM, VICTORY, Ranger3D Nomad, VYPER, SmartSpice, PSTATS, UTMOST IV, Measure, DISCOVERY, MERCURY, Optolith, TCAD Driven CAD, TonyPlot3D, RESILIENCE, Flash, ATHENA Interpreter, Interactive Tools, DeckBuild, DevEdit, ANALOG EXPRESS, CELEBRITY, SSuprem3, ATLAS, ATLAS Interpreter, Luminous2D/3D, MC Implant, S-Pisces, TonyPlot, FastLargeSignal, SmartStats, Ferro, DevEdit3D, Interpreter, Quantum2D/3D, SDDL, Circuit Optimizer, MaskViews, TFT2D/3D, Radiant, SSuprem4, Elite, FastBlaze, Mocasim, Silicides, MC Depo/Etch, FastNoise, Clarity, Blaze/Blaze3D, Device3D, Frontier, TwinSim, MixedMode2D/3D, VCSELS, Maverick, Envoy, Giga2D/3D, FastGiga, Guardian, Scout, FastMixedMode, Laser, Dragon, Expert, Spirit, Beacon, Savage, Harm, Zenith, Vision, Scholar, SN, UTMOST, UTMOST II, UTMOST III, UTMOST IV, PROMOST, SPAYN, ExpertViews, UTMOST IV Fit, FastSpice, Twister, Blast, MixSim, SmartLib, TestChip, Promost-Rel, RelStats, RelLib, Ranger, LISA, QUEST, EXACT, CLEVER, STELLAR, HIPEX-RCR, HIPEX-Net, HIPEX-RC, Connecting TCAD to Tapeout, and UTMOST IV Spice Modeling. All other product or company names are trademarks of their respective owners.

Hints, Tips and Solutions

Derek Kimpton, Applications Support Manager

Q. How can I create a Design Of Experiments (DOE) using *DeckBuild* with one or more variables specified in a single input file when I only have a single license ?

A. In *DeckBuild* it is possible to create a Design Of Experiments (DOE) using ANY variable or variables that were specified in the input file using the “set” statement (Linux or Unix platforms only).

The command line allows the user to set the total number of values for each variable, their minimum and maximum values and the manner in which each variable is swept. The variables can be swept linearly, or exponentially or a number of fixed data values can be listed manually.

The DOE function in *DeckBuild* will automatically create a complete DOE of every combination of variable and run each input file serially.

If the user does not wish to run every combination but is only interested in certain combinations, it is usually possible to achieve this by making multiple “parameter” statements. The format of these statements is described below.

Since the “set” statement is an existing syntax within *DeckBuild*, the user can utilize existing input files that already contain set statements to define variable quantities, to create a Design Of Experiments, without changing their existing input file at all.

To create a DOE, a separate but very simple control file is written, which specifies the input file for the DOE, then simply specifies the min, max and range (or list) required for the DOE for each variable that is required in the DOE. You can specify as few or as many variables to be included in the DOE as you desire. It does not matter what the default values of these set statement variables are in the original input file, their values in the DOE are solely determined by the control file. A simple example below describes how it works.

A quick word of warning is appropriate here, and that is, if the user wishes to save a separate structure or log file for each DOE entry, the name of that structure or log file needs to be dependent on the values of the variable in the DOE, otherwise, it will simply be over-written by

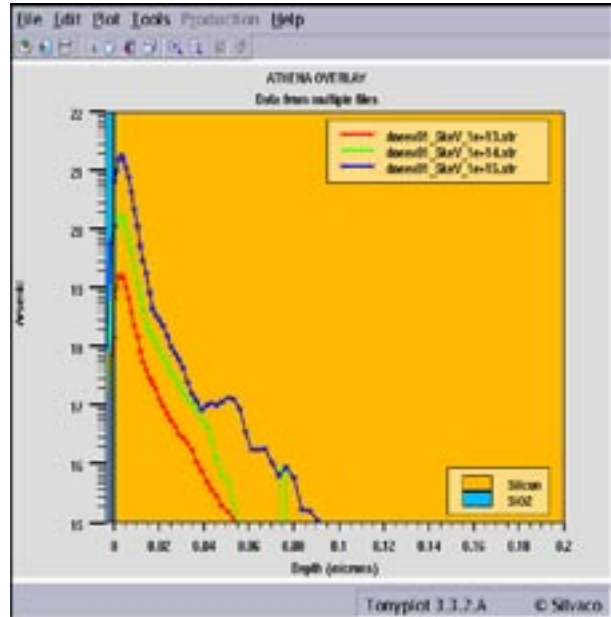


Figure 1.

each successive run. For example, if one of the variables in the DOE was “implant_energy” and it is desired to save a separate structure for each value of implant energy in the DOE, save a structure file called:

```
$(implant_energy)_keV.str  
and not  
implant.str
```

The structure file called `implant.str` will be over-written after each run of the DOE, because its name doesn't change with the changing values in the DOE. The structure file called `$(implant_energy)_keV.str` will be saved as `10_keV.str` for an implant energy of 10keV or `35_keV.str` for an implant of 35keV etc, thus a unique and identifiable structure file is saved for each value of implant energy in the DOE. A similar method for uniquely defining log files etc also needs to be used.

DOE Example

Let's take a simple example of an implant statement in an input file where implant dose and energy are the desired

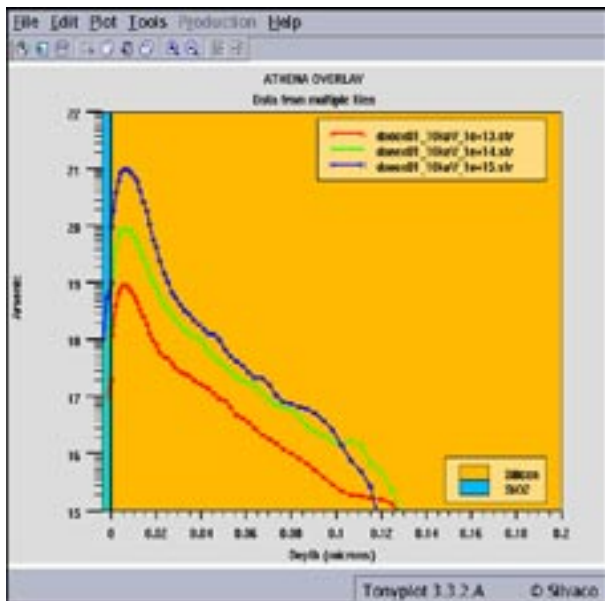


Figure 2.

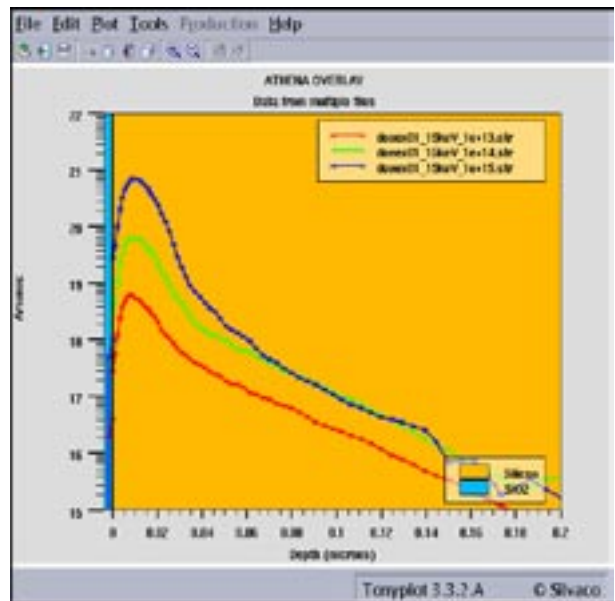


Figure 3.

variables in the DOE. The relevant lines in the original input file called "implant.in" are:-

```
set energy=5
set dose=1e13
implant arsenic dose=$dose \
  energy=$energy tilt=7 rot=27
```

As mentioned above, it doesn't actually matter what the defined "set values are in the original input file because these are defined in the DOE control file.

Now the user writes a very simple control files to control the values of implant dose and energy required in the DOE. An example control file is given below:

```
#####
go internal

load infile=implant.in

sweep parameter=dose type=power \
  range="1e13, 1e15, 3" parameter=energy \
  type=linear range="5, 15, 3"

quit
#####
```

Simply load this control file into *DeckBuild* and run it, making sure that the file called "implant.in" in this ex-

ample is also in the same directory. The control file will run every combination of implant doses of:

```
1e13, 1e14 and 1e15/cm2 for energies of :
5, 10 and 15keV
```

The same DOE could be specified using the "list" feature for either the dose, energy or both. If the "list" feature was used for energy, the syntax would be:

```
sweep parameter=dose type=power
range="1e13, 1e15, 3" \

parameter=energy type=list data="5, 10, 15"
```

The results of this simple DOE are shown in figures 1 thru 3. A similar example is demonstrated in the *DeckBuild* examples pull down menu under the heading "DOE: Design of Experiments Examples". If your Linux or Unix version of *DeckBuild* does not have this feature, please contact your account manager and request an update.

Call for Questions

If you have hints, tips, solutions or questions to contribute, please contact our Applications and Support Department
 Phone: (408) 567-1000 Fax: (408) 496-6080
 e-mail: support@silvaco.com

Hints, Tips and Solutions Archive

Check our our Web Page to see more details of this example plus an archive of previous Hints, Tips, and Solutions
www.silvaco.com

Join the Winning Team!

- PROCESS AND DEVICE APPLICATION ENGINEERS
- SPICE APPLICATIONS ENGINEERS
- CAD APPLICATIONS ENGINEERS
- SOFTWARE DEVELOPERS

EMAIL TO: CAREERS@SILVACO.COM



SILVACO

INTERNATIONAL

USA Headquarters:

Silvaco International

4701 Patrick Henry Drive, Bldg. 2
Santa Clara, CA 95054 USA

Phone: 408-567-1000

Fax: 408-496-6080

sales@silvaco.com

www.silvaco.com

Contacts:

Silvaco Japan

jpsales@silvaco.com

Silvaco Korea

krsales@silvaco.com

Silvaco Taiwan

twsales@silvaco.com

Silvaco Singapore

sgsales@silvaco.com

Silvaco UK

uksales@silvaco.com

Silvaco France

frsales@silvaco.com

Silvaco Germany

desales@silvaco.com

*Products Licensed through Silvaco or e*ECAD*

